Global column-averaged methane mixing ratios from 2003 to 2009 as derived from SCIAMACHY: Trends and variability

C. Frankenberg,[1,2] I. Aben,[1] P. Bergamaschi,[3] E. J. Dlugokencky,[4] R. van Hees,[1] S. Houweling,[1,5] P. van der Meer,[1] R. Snel,[1] and P. Tol[1]

Received 30 July 2010; revised 19 November 2010; accepted 30 November 2010; published 17 February 2011.

[1] After a decade of stable or slightly decreasing global methane concentrations, ground-based in situ data show that CH_4 began increasing again in 2007 and that this increase continued through 2009. So far, space-based retrievals sensitive to the lower troposphere in the time period under consideration have not been available. Here we report a long-term data set of column-averaged methane mixing ratios retrieved from spectra of the Scanning Imaging Absorption Spectrometer for Atmospheric Cartography (SCIAMACHY) instrument onboard Envisat. The retrieval quality after 2005 was severely affected by degrading detector pixels within the methane $2\nu_3$ absorption band. We identified the most crucial problems in SCIAMACHY detector degradation and overcame the problem by applying a strict pixel mask as well as a new dark current characterization. Even though retrieval precision after the end of 2005 is invariably degraded, consistent methane retrievals from 2003 through 2009 are now possible. Regional time series in the Sahara, Australia, tropical Africa, South America, and Asia show the methane increase in 2007–2009, but we cannot yet draw a firm conclusion concerning the origin of the increase. Tropical Africa even seems to exhibit a negative anomaly in 2006, but an impact from changes in SCIAMACHY detector degradation cannot be excluded yet. Over Assakrem, Algeria, we observed strong similarities between SCIAMACHY measurements and ground-based data in deseasonalized time series. We further show long-term SCIAMACHY xCH_4 averages at high spatial resolution that provide further insight into methane variations on regional scales. The Red Basin in China exhibits, on average, the highest methane abundance worldwide, while other localized features such as the Sudd wetlands in southern Sudan can also be identified in SCIAMACHY xCH_4 averages.

Citation: Frankenberg, C., I. Aben, P. Bergamaschi, E. J. Dlugokencky, R. van Hees, S. Houweling, P. van der Meer, R. Snel, and P. Tol (2011), Global column-averaged methane mixing ratios from 2003 to 2009 as derived from SCIAMACHY: Trends and variability, *J. Geophys. Res.*, *116*, D04302, doi:10.1029/2010JD014849.

1. Introduction

[2] Atmospheric CH_4 is the most important anthropogenic greenhouse gas (GHG) after CO_2, exhibiting both a direct and an indirect radiative forcing [*Forster et al.*, 2007]. Since preindustrial times, its atmospheric abundance has more than doubled, showing a rapid increase until 2000 with stable mixing ratios from 2000 through 2006 [*Dlugokencky et al.*, 2003]. Ground-based measurements, however, indicate that atmospheric CH_4 increased again significantly in 2007 and 2008 [*Rigby et al.*, 2008; *Dlugokencky et al.*, 2009]. This increase corresponds to a source-sink imbalance of approximately 20 Tg/yr, and so far a combination of enhanced high-latitude emissions (due to an exceptionally warm summer of 2007) and tropical emissions (more rainfall in 2008) are being hypothesized as the causes [*Dlugokencky et al.*, 2009]. Ground-based measurements from NOAA's South Pole Observatory, as shown in Figure 1, are an ideal proxy for the global background concentration on annual timescales and indicate a further increase in 2009. None of the anomalies observed in the past 25 years [*Dlugokencky et al.*, 2003] have lasted this long, and this sets the current anomaly apart and warrants further investigation, especially with respect to future predictions.

[3] The Scanning Imaging Absorption Spectrometer for Atmospheric Cartography (SCIAMACHY), launched aboard the European research satellite Envisat in March 2002, enables methane retrievals with high sensitivity near

[1]SRON Netherlands Institute for Space Research, Utrecht, Netherlands.
[2]Now at Jet Propulsion Laboratory, California Institute of Technology, Pasadena, California, USA.
[3]Institute for Environment and Sustainability, European Commission Joint Research Centre, Ispra, Italy.
[4]NOAA Earth System Research Laboratory, Global Monitoring Division, Boulder, Colorado, USA.
[5]Institute for Marine and Atmospheric Research Utrecht, Utrecht, Netherlands.

0148-0227/11/2010JD014849

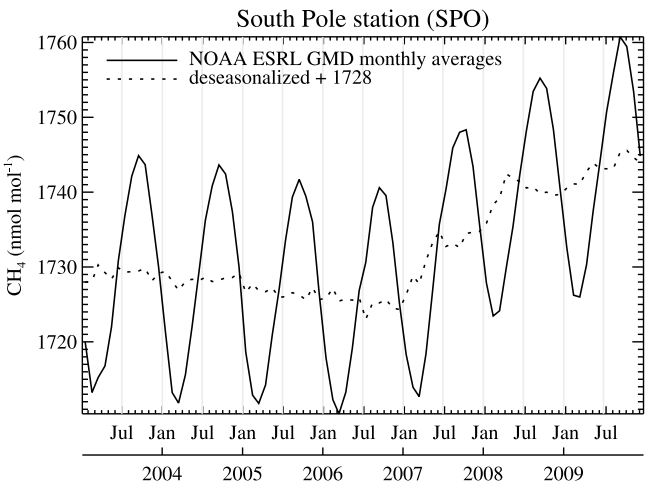

Figure 1. Ground-based measurements from 2000 through 2009 at the NOAA Earth System Research Laboratory Global Monitoring Division South Pole Observatory, 2810 masl. For deseasonalizing, the monthly means averaged over 2003–2005 were subtracted from each individual monthly mean.

the ground. Those measurements have proven to be a valuable additional constraint for the determination of global methane sources [*Bergamaschi et al.*, 2007, 2009], especially in regions devoid of ground-based measurements. Recently, we reported a major revision of CH_4 retrievals [*Frankenberg et al.*, 2008a], resulting in significantly lower column-averaged CH_4 mixing ratios, especially in the tropics (compared with the earlier retrieval versions). This revision corrected for systematic errors that had been identified in the spectroscopic parameters of CH_4 [*Frankenberg et al.*, 2008b] and H_2O vapor [*Frankenberg et al.*, 2008a]. *Bergamaschi et al.* [2009] reported the first top-down inversions using the new data set in the TM5 chemistry transport model and a 4-D variational (4DVAR) inversion scheme. Owing to the complexity of methane retrievals from SCIAMACHY, operational real-time data products are not available and scientific data products from various institutions have so far only covered the time period until the end of 2005 [*Frankenberg et al.*, 2008a; *Schneising et al.*, 2009], thus only covering a time period of relatively stable, in terms of annual variations, methane concentrations. Instrumental problems, specifically the degradation of crucial detector pixels of the SCIAMACHY spectrometer in the short-wave infrared, have impeded the analysis since 2005.

[4] The main purpose of this work is to enable a long-term time series of SCIAMACHY data which can be used to investigate interannual variations as well as long-term mean methane abundance. In section 2, we analyze SCIAMACHY-specific retrieval problems and present a method allowing robust retrievals from 2003 through December 2009. Section 3 describes the impact of the retrieval and compares it with the previous version. Section 4 describes differences between total column, surface, and stratospheric variations. In section 5, we show long-term deseasonalized time series from SCIAMACHY for different geographical regions and compare them with ground-based stations. Section 6 briefly describes current bottom-up inventories of anthropogenic methane emissions. In section 7, we discuss the long-term average of methane from SCIAMACHY at high spatial resolution before we summarize our results in section 8.

2. SCIAMACHY-Specific Retrieval Issues

[5] SCIAMACHY measurements of CH_4 and CO_2 are both based on short-wave infrared spectra recorded in the 1.5–1.7 μm range by SCIAMACHY's channel 6. It is important to recall that CH_4 presented here and in previous publications relies on the proxy method, using concurrent CO_2 retrievals to account for changes in the light path distribution [*Frankenberg et al.*, 2005]. Hence, ancillary information on the CO_2 column average are needed for the accurate determination of the CH_4 column average. *Butz et al.* [2010] provide a thorough test of the proxy method and compare it with full physics retrievals which might be possible in future missions.

[6] The SWIR channel for CH_4 and CO_2 retrievals employs indium gallium arsenide detectors (InGaAs; EPITAXX, New Jersey) specifically developed and qualified for SCIAMACHY [*Hoogeveen et al.*, 2001]. Because of the sensitivity drop of standard InGaAs elements at about 1.7 μm, the longer wavelength part of channel 6, denoted channel 6+, is doped with higher amounts of indium. This results in higher dark currents and, as experienced so far, more frequent radiation damage and concurrent degradation of detector pixels [*Kleipool et al.*, 2007]. While CO_2 retrievals performed in channel 6 are not affected and so far have remained stable over the entire SCIAMACHY mission, degradation affects methane retrieval performed in channel 6+. Degradation may arise in different forms, the worst case being pixels entirely unresponsive, hence labeled dead. Intermediately degraded pixels, labeled bad, can exhibit multimodal distributions in the dark current (measured signal in the absence of illumination). The actual dark current can then exhibit random, discrete switching between the modes (so-called random telegraph signal (RTS)). A simple increase in detector noise is a further mild form of degradation.

[7] Figure 2 shows a typical SCIAMACHY spectrum over the Sahara as well as the most important detector pixels used for methane retrieval as they cover the strong $2\nu_3$ methane Q branch. (Pixel numbering starts from the beginning of channel 6+.) Figure 2 (bottom) depicts the dark current characteristics of the three most important pixels recorded in each orbit during an eclipse. Two orbits have been chosen to exemplify the degradation in time: orbit 15000 (January 2005, before degradation) and orbit 31000 (February 2008, after degradation). As can be seen, pixels 97 and 99 feature RTS behavior (bimodal distribution) as well as increased noise in dark current (increased spread in the distribution). Pixel 98, however, is only affected by an increase in noise, which started in November 2005. To avoid an impact of RTS pixels on the retrieval, we performed a reanalysis of the entire 2003–2009 period after excluding pixels 97 and 99 to ensure optimal consistency throughout the period. In the particular case of Figure 2, a standard deviation in the dark current of about 25 BU (at a signal of about 9000 BU) would yield a signal-to-noise ratio of 360, just taking into account the dark current noise and a

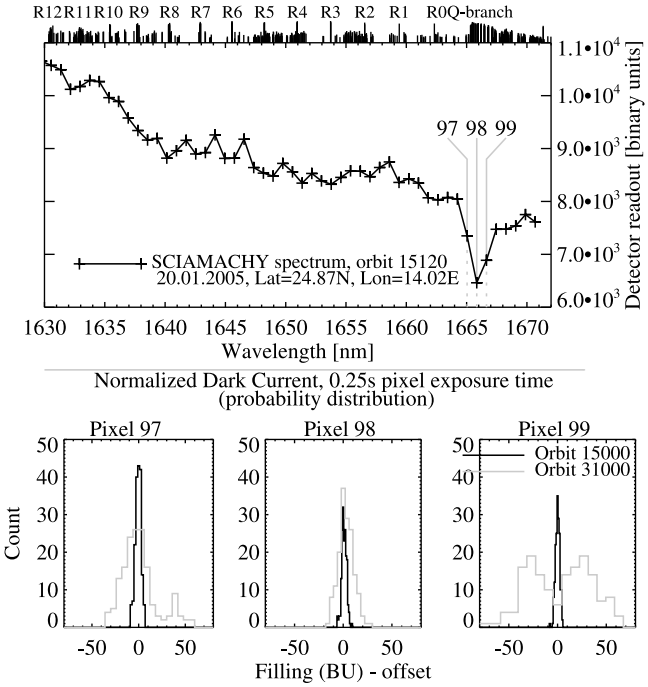

Figure 2. (top) SCIAMACHY earthshine spectrum (not radiometrically calibrated) for a bright surface on 20 January 2005. Pixels 97–99, indicated as pixel positions within channel 6+ of SCIAMACHY, cover the Q branch of the $2\nu_3$ band of methane and provide the highest sensitivity for the methane retrieval. Stick spectrum indicates line intensities and assignments of the methane $2\nu_3$ band. (bottom) Frequency distribution of dark current measurements taken in eclipse for pixels 97–99 in orbit 15000 (11 January 2005) and orbit 31000 (3 February 2008). The *x* axis shows dark current measurements in raw detector units (BU, binary units; detector readout before any calibration steps are taken) centered at zero, since the absolute value of the dark current slightly changes in time but we only want to depict variability.

very bright surface (Sahara). Currently, we only use spectra with a minimal readout of 1500 BU. At this readout level, it becomes clearly obvious that dark current noise, not depending on absolute signal level, can become a dominant noise term affecting retrieval precision. Any systematic error in dark current, as can happen for RTS pixels, will lead to an upward or downward shift of the calibrated spectrum, thereby affecting retrieval accuracy if the respective pixel covers a methane absorption line.

[8] Further, we implemented a more robust dark current determination scheme that allows the application of RTS pixels with one dominant dark current state [*Sheather and Jones*, 1991]. So far, this procedure works correctly only for pixel 98, but pixels 97 and 99 switch dark current states too frequently.

[9] Despite the efforts to improve the dark current corrections, spurious measurements with significant differences in methane column abundance can still be encountered. These retrievals can be attributed to anomalous dark currents, deviating several σ from the mean state. It is not possible to discard the measurements on the basis of reduced fit residuals, since those were hardly affected. In most cases, few measurement states within an orbit are affected by this behavior, but they can still strongly bias averaged xCH_4 maps. So far, those were discarded on the basis of visual inspection of individual orbits, a method which is both cumbersome and not based on quantitative criteria. We find that these outliers are mainly caused by outliers in the dark current of pixel 98. Because of the alternating limb-nadir scanning of SCIAMACHY, we can use so-called last-limb measurements with a tangent height of about 250 km (hence dark) as quality criteria for the dark current correction in orbit. We have set thresholds on the mean, the standard deviation, and the orbital variation within those limb states to filter spurious orbits. After this procedure, no additional manual filtering of orbits is required.

3. Comparison With Previous Retrieval Version

[10] Because of the neglect of crucial detector pixels 97 and 99, a systematic difference with respect to the previous retrieval version [*Frankenberg et al.*, 2008a] can be introduced. Figure 3 shows the systematic difference between retrievals neglecting detector pixels 97 and 99 and using them (with all other parameters kept the same). Apart from an approximate 20 ppb offset between the versions, most variations are well below 1%, i.e., about 18 ppb. However, slightly but systematically higher tropical values can be observed when neglecting pixels 97 and 99. This might be related to interference with atmospheric water vapor, as discussed for the previous version by *Frankenberg et al.* [2008a]. It is feasible that the omission of pixels 97 and 99 again creates either a latitudinal and surface albedo-related bias or a slight interference with water vapor, as there is less spectral information to discern between the variations in methane and water vapor. Hence, care has to be taken when using this new long-term data set in source inversions, since tropical emission might be overestimated in that case. However, we focus here on interannual variations in specific regions which are less sensitive to these biases. A further analysis of potential interference and other systematic errors in SCIAMACHY data will be performed when retrievals from the Japanese Greenhouse Gases Observing Satellite (GOSAT) [*Kuze et al.*, 2009] using the same proxy method become available. This will also provide a deeper understanding of SCIAMACHY data in hindsight, as the high spectral and spatial resolution of GOSAT as well as its capability to retrieve the CO_2 proxy in a band spectrally closer to CH_4 will result in far fewer systematic errors and virtually exclude any potential spectroscopic interference. This, however, is beyond the scope of our current study.

4. Interpretation of Column-Averaged Mixing Ratios Derived From Space

[11] Before showing column-averaged mixing ratios derived from SCIAMACHY spectra, we briefly discuss the interpretation of this quantity as it sometimes leads to confusion and must not be interpreted in the same way as surface mixing ratios. One of the most important factors controlling the column-averaged mixing ratios is the meth-

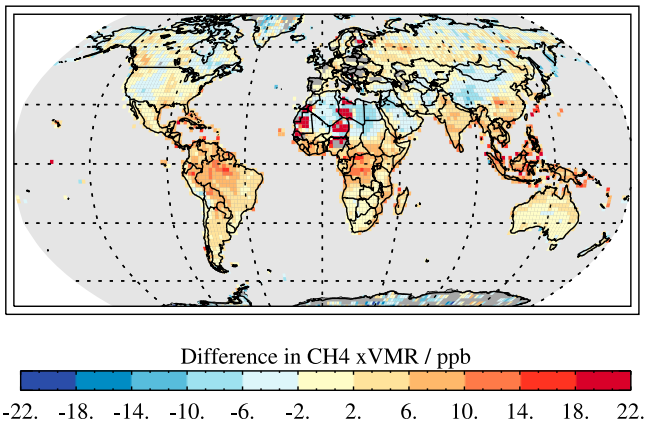

Figure 3. Difference between retrieval versions using detector pixels 97 and 99 (see Figure 2) and an identical version with those pixels flagged as dead in the retrieval (displayed is "without 97/99" minus "with 97/99" minus "20 ppb offset").The comparison is shown for a 2004 average when pixels 97 and 99 were still working properly most of the time. Over the Sahara, some outlier values can be clearly observed (in the shape of a typical SCIAMACHY nadir observation pattern due to the nadir-limb switch). These are retrievals where one of the pixels, 97 or 99, already behave anomalously for a short period of time (intentionally left in this comparison).

ane abundance in the stratosphere. Because of slow mixing in the stratosphere, methane is typically far less abundant than in the troposphere and its concentration depends on the age of air. Since the relative contribution of the stratosphere to the vertically integrated mass of an atmospheric column depends on tropopause height, tropopause height exhibits a positive correlation with the column-averaged methane mixing ratio. This is of prime importance when considering latitudinal gradients in general and might cause problems at sharp polar vortex edges unresolved in the atmospheric model being used to invert methane fluxes from SCIAMACHY measurements. Seasonal cycles in specific regions might also be affected, causing a decoupling of surface and column-averaged mixing ratios, especially in remote regions devoid of methane sources.

[12] Since the near-infrared satellite retrievals do not provide profile information, we use a model to elucidate methane variability at different height layers and also to act as a transfer standard between surface and total column measurements. We use the TM5-4DVAR model fields, which have been optimized using global background monitoring sites and enable us to relate the high-accuracy surface measurements to column-averaged mixing ratios in a consistent way. The TM5-4DVAR model is described in detail by *Meirink et al.* [2008], and subsequent developments are described by *Bergamaschi et al.* [2009] and *Bergamaschi et al.* [2010]. TM5 is an offline transport model [*Krol et al.*, 2005] driven by meteorological fields from the European Centre for Medium Range Weather Forecasts (ECMWF) Integrated Forecast System (IFS) model. For the present study, we apply the ERA-Interim meteorological fields, a reanalysis of the period from 1989 until the present, to ensure consistent meteorological fields over the time period analyzed (2003–2009). We employ the standard TM5 version (TM5 cycle 1) with 25 vertical layers, defined as a subset of the 60 layers used in the ECMWF IFS model for the ERA-Interim reanalysis, and apply a horizontal resolution of 6° × 4°.

[13] Figure 4 provides an example of modeled methane abundance over the Sahara in different height layers. As can be seen, seasonal variations at different height layers can show opposite behavior, all affecting the total column average that therefore exhibits a different seasonal cycle than surface concentrations. Interpretation of total column averages without considering an atmospheric transport model should thus be done carefully. In an inverse modeling approach using in situ data, the pressure level of the station has to be taken into account, but the mountain itself will not be resolved by coarse resolution global models, potentially causing representativeness errors.

[14] Figure 5 shows the differences between annually averaged surface measurements and total column averages on the global scale. Surface concentrations show, as expected, higher variations and are also higher than the total column average in most cases. The interhemispheric gradient at the Intertropical Convergence Zone (ITCZ) is far more distinct as the stratospheric latitudinal gradient smooths out this feature in the total column average. Similarly, the land-sea contrast due to continental emissions is smoother. Over regions with high emissions, surface mixing ratios can exceed the column average by more than 200 ppb, while in some cases, such as over tropical ocean sites, the column average can be slightly higher than surface abundance. This may be caused by uplifted emissions in continental outflow regions (in conjunction with a high tropopause, such as in the tropics). These are just examples of the intricacies when interpreting column-averaged mixing ratios. Atmospheric models used to invert for methane emissions on the basis of SCIAMACHY data should thus properly simulate stratospheric variations. This might be especially important at higher latitudes [*Bergamaschi et al.*, 2009].

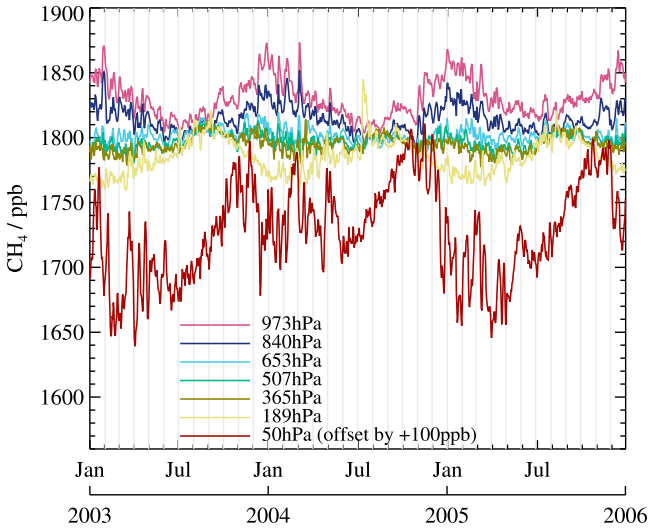

Figure 4. Time series of the TM5 model at different model layers over the Sahara (15°N–30°N, 0°E–13°E).

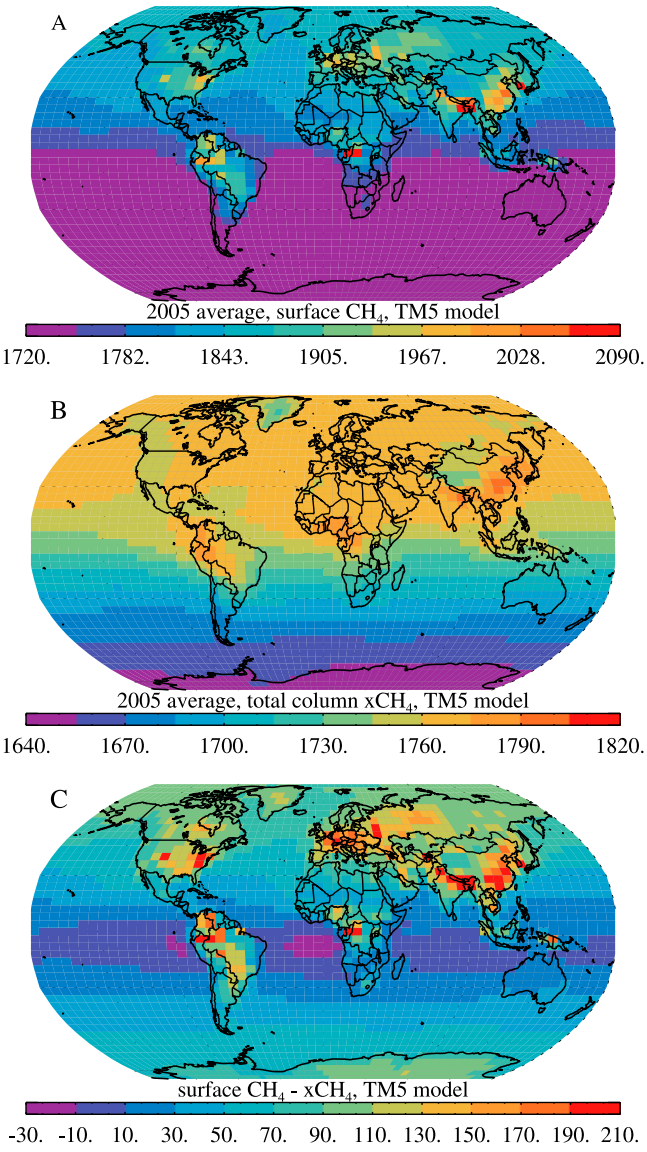

Figure 5. Illustration of differences between column-averaged and surface mixing ratios (based on the TM5 model). (a) Yearly average (2005) of surface mixing ratios obtained from the TM5 model. (b) Corresponding column average mixing ratios for the same time period. (c) Difference between surface and column-averaged mixing ratios.

[15] A further factor of consideration is surface elevation: The relative stratospheric contribution to the mass of an atmospheric column increases with surface elevation as mountains basically reduce the tropospheric fraction. Hence, total column averages over mountain ranges are typically reduced. This may cause problems if the atmospheric model used for the inversion cannot resolve the mountain range at coarse resolution. Hence, we provide the mean and the standard deviation of surface elevation within each SCIAMACHY ground pixel as ancillary information to account for possible model measurement mismatches in topography.

[16] As we have seen, both troposphere and stratosphere often exhibit rather smooth seasonal variations due to seasonal variations in tropopause height, OH radicals, and methane emissions. Deviations from typical seasonal cycles are likely caused by emission or wind field anomalies and should therefore mostly affect the troposphere. Hence, anomalies from the typical seasonal cycle in total column and surface methane are expected to show better agreement than the seasonal cycle itself. We exploit and strengthen this assumption in the following section.

5. Multiyear Column-Averaged Mixing Ratios of Methane Derived From SCIAMACHY

[17] Using the improved bad pixel mask, dark current correction, and orbit filtering as outlined in section 1, we reanalyzed SCIAMACHY spectra (processor version 6.03 only) from 2003 through 2009. Figure 6 shows the 2003–2008 global average (land only) of these measurements gridded on a 1/3° by 1/3° scale without further smoothing. (That is, neighboring grid cells do not share information other than a potential overlap of 60 × 30 km ground pixels.) Despite the high spatial resolution, the variations appear very smooth owing to the ≈8 year lifetime of methane [*Lelieveld et al.*, 1998]. Most distinct variations are caused by surface elevation (as outlined in section 4), such as the sharp edge at the Himalayan foothills, the Andes Mountains, or the Rocky Mountains. Before discussing specific regions in the long-term mean, we focus on the time evolution in discrete latitude bins as well as over specific areas that are indicated by the white boxes in Figure 6. (Only measurements over the continents are taken into account.) Measurements from selected ground-based air sampling sites that are part of the NOAA Earth System Research Laboratory (ESRL) global cooperative air sampling network are used in this study and indicated in Figure 6 as well.

[18] Figure 7 shows latitudinal monthly averages of all SCIAMACHY retrievals over land from 2003 through 2009. Figure 7 (top) shows absolute xVMR values, while Figure 7 (bottom) depicts anomalies by subtracting a mean seasonal cycle calculated on the basis of the years 2003 through 2005. The renormalization of the CH_4-to-CO_2 ratio [*Frankenberg et al.*, 2006; *Frankenberg et al.*, 2005] retrieved by SCIAMACHY has been performed with CarbonTracker data [*Peters et al.*, 2007] for 2003 through 2007. For 2008 and 2009, we applied CarbonTracker column-averaged mixing ratios from the same locations (and times) in 2007, but these account for ≈0.4% annual increase in total column CO_2 (determined from the increase in total column CO_2 from 2003 through 2007). Systematic errors in modeled CO_2, one of the prime uncertainties in methane retrieval, are therefore expected to be higher in 2008 and 2009. The good correspondence with TM5 and NOAA suggests that the error due to CO_2 cannot be very large. From Figure 7 (bottom), it appears that tropical abundance in 2006 was significantly lower than before and rebounded at the end of 2006. Apart from this feature, there is no latitudinal band distinguishable in terms of an apparent anomaly at the onset of the global increase starting in early 2007. We discuss the tropical anomaly in 2006 in more detail in the following discussion of time series over Africa and South America. Since the retrieval quality degraded at the end of 2005, a tropical bias in 2006 cannot be fully excluded. However, we show later that the negative anom-

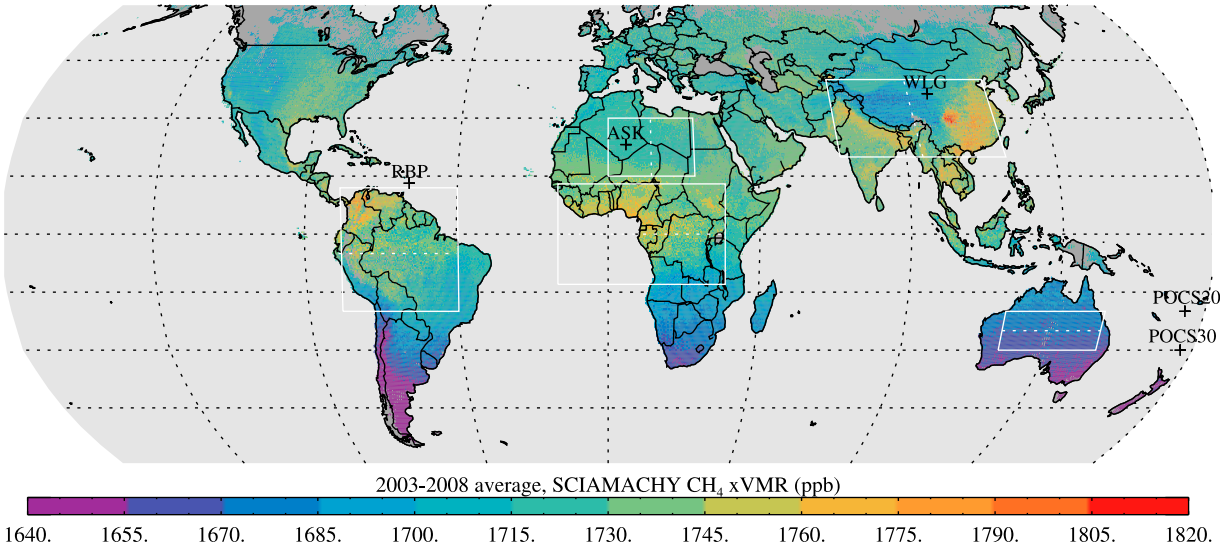

Figure 6. The 2003–2008 average of methane column-averaged mixing ratios retrieved from SCIAMACHY. Gridding has been performed on 1/3° by 1/3°. White boxes indicate regions where a separate time series of averaged SCIAMACHY data are shown in Figures 8–12. (The dashed white line indicates the east-west or north-south division in the respective time series figures.) The locations of some NOAA ground-based cooperative air sampling sites are shown as crosses.

aly is not observed in this magnitude in South America, which provides an argument against a bias as the only explanation.

[19] We also compare SCIAMACHY time series with colocated model simulations on the basis of the TM5-4DVAR inverse modeling system. The 4DVAR optimization technique minimizes iteratively a cost function, taking into account an a priori estimate of the emissions on the basis of the emission inventories used by *Bergamaschi et al.* [2010]. We assimilate only surface observations from the NOAA ESRL global cooperative air sampling network [*Dlugokencky et al.*, 2003; *Dlugokencky et al.*, 2009] using the same set of global background monitoring sites employed by *Bergamaschi et al.* [2009]. For computational reasons, the inversion is split into 15 month periods with 3 month overlaps using the optimized 3-D fields at the beginning of each year from the previous inversion. We use precalculated monthly OH fields on the basis of Carbon Bond mechanism 4 chemistry [*Bergamaschi et al.*, 2009], but do not take into account any potential interannual variability of OH in this study. The major purpose of using the inverse model simulations is to provide 3-D fields consistent with the NOAA surface observations as a reference point for comparisons with the satellite retrievals rather than analyzing the interannual variability of emissions in detail. All TM5 model simulations shown here are column-averaged mixing ratios, not taking the averaging kernel of SCIAMACHY into account.

[20] In the following discussion, we show time series over specific locations and compare anomalies with ground-based measurements as well as the model simulations on the basis of the TM5-4DVAR model described above.

[21] Figure 8 shows the time series of SCIAMACHY retrievals from 2003 through 2009 (region outlined in Figure 6). Over the Sahara, SCIAMACHY retrievals are very reliable for two reasons: First, the high surface albedo provides a very good signal-to-noise ratio, and second, frequent cloud-free scenes allow the computation of robust statistical averages. Figure 8 (top) shows the monthly averages as well as the frequency distribution of all SCIAMACHY measurements in 10 day temporal bins. It is apparent that the spread of the frequency distribution increases suddenly in November 2005, owing to the degradation (in terms of dark current noise) of the crucial pixel 98 as explained in section 2. A systematic change in SCIAMACHY methane column averages, however, cannot be observed after degradation. Since total column averages cannot be directly compared with near-surface measurements and since the observed increases in 2007 and 2008 [*Rigby et al.*, 2008; *Dlugokencky et al.*, 2009] are smaller than seasonal variations, we calculate deseasonalized monthly anomalies in the following way: The mean monthly value calculated from 2003 to 2005 is subtracted from each monthly mean estimate. This procedure is applied to both satellite and surface monthly average concentration estimates. Figure 8 (bottom) shows these anomalies separately for the east and west part of the averaging region. In addition, we show TM5 column-averaged mixing ratios (in red are anomalies calculated in the same way as for SCIAMACHY) as well as monthly anomalies of NOAA air samples collected at Assakrem, Algeria (ASK; situated on the western part of the averaging region). Striking similarities between ground-based, TM5, and SCIAMACHY monthly anomalies can be observed: There is a common decrease from September 2003 through January 2005 and even some month-to-month variations, such as in the beginning of 2006, can be observed in both time series. In terms of anomalies, satellite and ground-based data can thus exhibit substantial correlations, paving the way for new validation methods. However, it has to be noted that the Sahara and Assakrem locations are ideal sites for comparisons, since (1) SCIAMACHY has a high signal-to-noise ratio in this

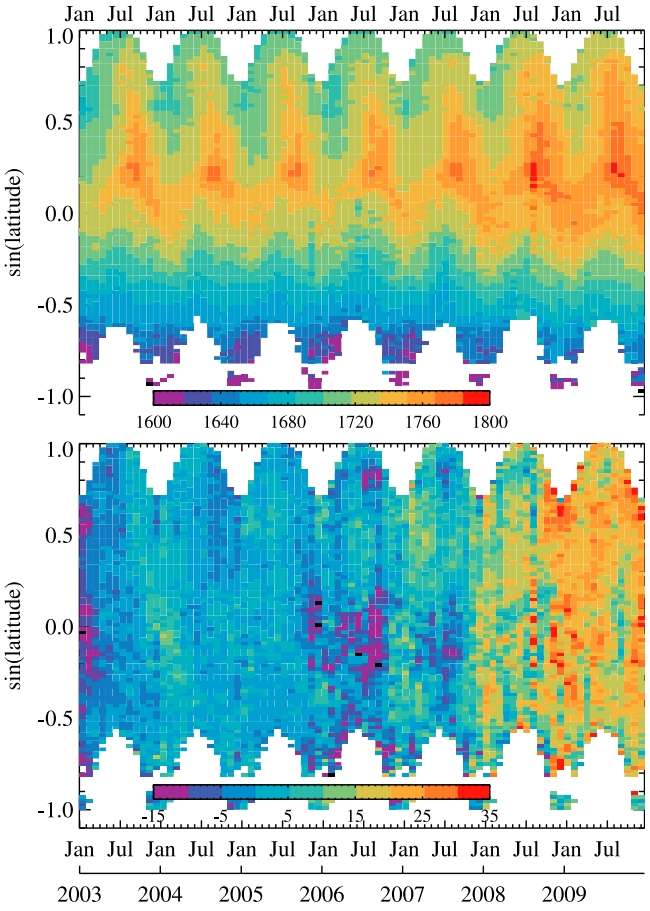

Figure 7. (top) Latitudinal monthly averages (land only) of all SCIAMACHY xCH_4 retrievals from January 2003 through December 2009. (bottom) Deseasonalized time series for SCIAMACHY latitudinal averages. For deseasonalizing, the monthly means averaged over 2003–2005 were subtracted from each individual monthly mean in the respective latitude bins.

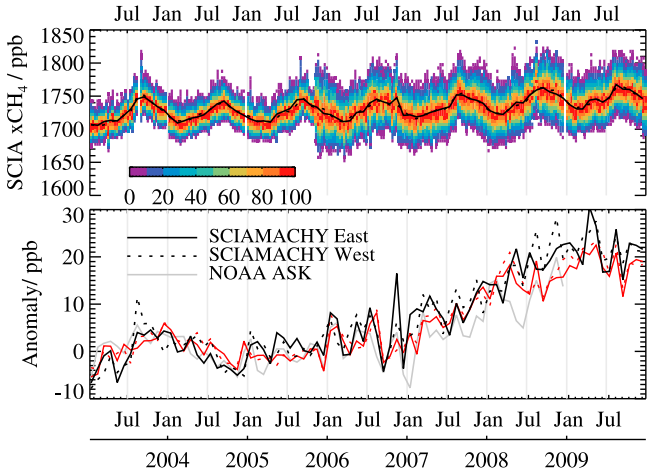

Figure 8. (top) Time series of SCIAMACHY xCH_4 from January 2003 through December 2009 over the Sahara. The black lines (continuous, eastern part; dotted, western part; regions are as indicated in Figure 6) are monthly means, while the normalized frequency distribution of all measurements within a 10 day time window is shown in colors. (Values below 5% are not plotted.) (bottom) Deseasonalized time series for SCIAMACHY and NOAA CH_4 measurements from Assakrem. For deseasonalizing, the monthly means averaged over 2003–2005 were subtracted from each individual monthly mean. For comparison, collocated TM5 model means are shown in red (continuous, eastern part; dotted, western part). Exact boundaries are latitude [15°, 30°] and longitude [0°, 26°].

region and (2) the ground-based site, devoid of local sources, is representative of a large region.

[22] Over the Sahara, the increases in 2007 and 2008 are clearly identified in SCIAMACHY data, with anomalies approaching 15 ppb at the end of 2008, consistent with ground-based measurements. Most monthly column anomalies are well within 5 ppb, being below 0.3% of the total column. This is an assurance of very high accuracy obtained from space over an ideal ground scene (with a nonideal and not dedicated greenhouse gas-detecting spectrometer). At this accuracy level, concurrent anomalies in CO_2, which is currently still being used as proxy for light path variations [*Frankenberg et al.*, 2006; *Frankenberg et al.*, 2005], can also play an important role if they are misrepresented in the applied CO_2 model being used for rescaling methane (here we used CarbonTracker; *Peters et al.* [2007]).

[23] Figure 9 shows the same time series as Figure 8 but for Australia. There are no NOAA ground-based observations within the averaged area, but we chose two Pacific Ocean sites at comparable latitudes (POCS20 and POCS30). While the increases in 2007 and 2008 can still be clearly observed, clear correlations between the time series are lacking, either because of low methane variability in this region or because of a regional mismatch between SCIAMACHY and the ground-based stations. An increased spread in

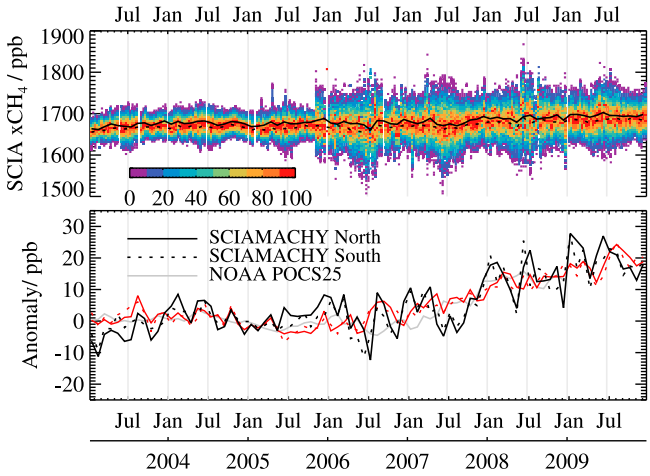

Figure 9. Same as Figure 8 but for SCIAMACHY averages over Australia divided into northern and southern parts (same for following captions) and two NOAA sampling locations in the Pacific Ocean. Exact boundaries are latitude [−30°, −20°] and longitude [120°, 150°].

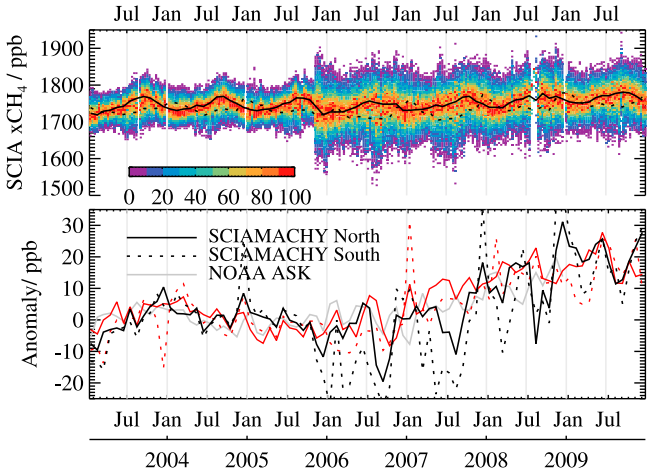

Figure 10. Same as Figure 8 but for SCIAMACHY averages over Africa. Exact boundaries are latitude [−13°, 13°] and longitude [−15°, 35°].

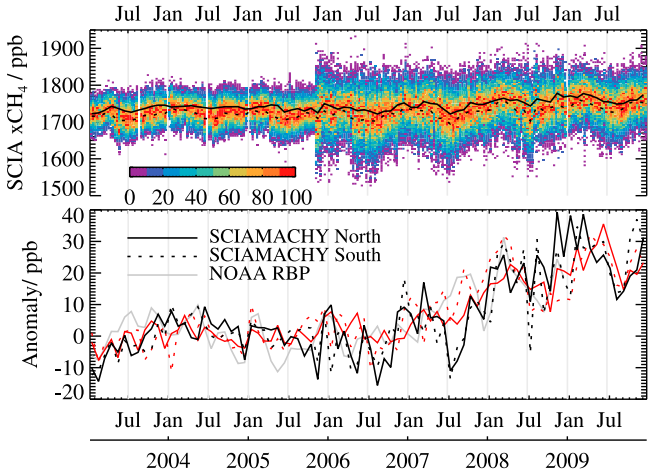

Figure 11. Same as Figure 8 but for SCIAMACHY averages over South America and NOAA CH_4 observations at Ragged Point, Barbados. Exact boundaries are latitude [−20°, 12°] and longitude [−80°, −45°].

retrieved xCH_4 in austral winter can be observed that is primarily attributable to higher solar zenith angles and a concurrent decrease in the signal-to-noise ratio.

[24] Figure 10 continues with a more interesting region with respect to methane emissions, namely, tropical Africa. The different seasonality of the northern versus the southern part of tropical Africa can be nicely observed in Figure 10 (top) (solid and dashed lines). Only in January does the southern part exhibit higher abundance than in the north, primarily due to shifts in rainfall patterns and associated wetland emissions [*Bloom et al.*, 2010]. The behavior between 2003 and 2005 looks very smooth and resembles the ground-based station at Assakrem. (No other stations are located nearby.) After 2005 and with the onset of the degradation of pixel 98, however, strong variations occur, but they are mostly negative anomalies, especially in the southern part of tropical Africa. This negative anomaly is not visible in the TM5-4DVAR model simulations. This could be due to the fact that remote surface observations used in the inversion are not very sensitive to tropical emissions, but it could also indicate some systematic bias of SCIAMACHY retrievals as a result of the pixel degradation. There are no obvious positive detectable spikes that could strongly support a hypothesis of tropical Africa's being the primary driver for the observed increase in global methane abundances. Only in January of 2008 and 2009 can anomalous values in southern tropical Africa be detected. Most negative anomalies center around the month of September in all years from 2006 to 2009, but with varying amplitude. The TM5 model also shows a small negative anomaly only at the end of 2006, but with a somewhat smaller amplitude than SCIAMACHY (and shifted by 1–2 months).

[25] In tropical South America, depicted in Figure 11 (top), total column variations in the southern and northern parts are much more similar than in Africa, most likely because of the lack of dominant north-south oriented seasonal variations in precipitation. The nearest ground-based station is at Ragged Point, Barbados. A small increase in the beginning of 2007 is observed, but it is followed by a negative anomaly in July. As in tropical Africa, there is no sudden or very anomalous event observed in tropical South America. Negative anomalies in the July–September period in 2006 and 2007 coincide with tropical Africa, but they exhibit a smaller amplitude. After the negative anomalies in 2006 and 2007, both tropical regions exhibit a strong increase in the anomalies and reach concentrations more comparable to the TM5 model.

[26] Only in East Asia, depicted in Figure 12, can enhanced values from mid-2006 through mid-2007 be observed, and they are in line with the TM5 model. They are slightly stronger in the eastern (Chinese) than in the western (Indian) part of the area under investigation. The ground-based observations from Mount Waliguan (China) do not show this anomaly in 2006 and 2007, but they show pro-

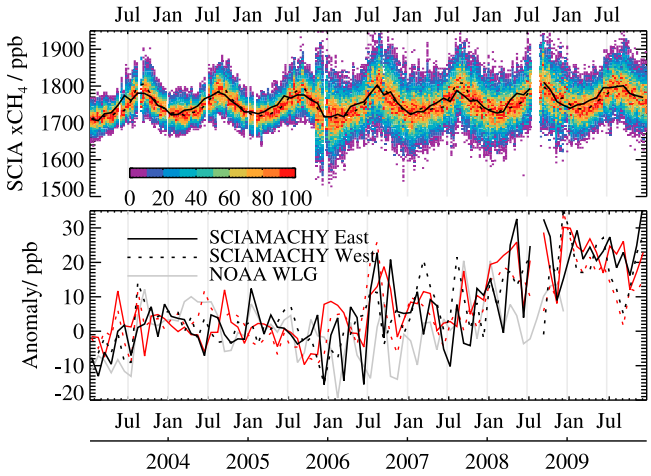

Figure 12. Same as Figure 8 but for SCIAMACHY averages over Asia (divided into eastern and western parts) and NOAA CH_4 observations at Mount Waliguan (operated by Chinese Academy of Meteorological Sciences). Exact boundaries are latitude [20°, 40°] and longitude [70°, 120°].

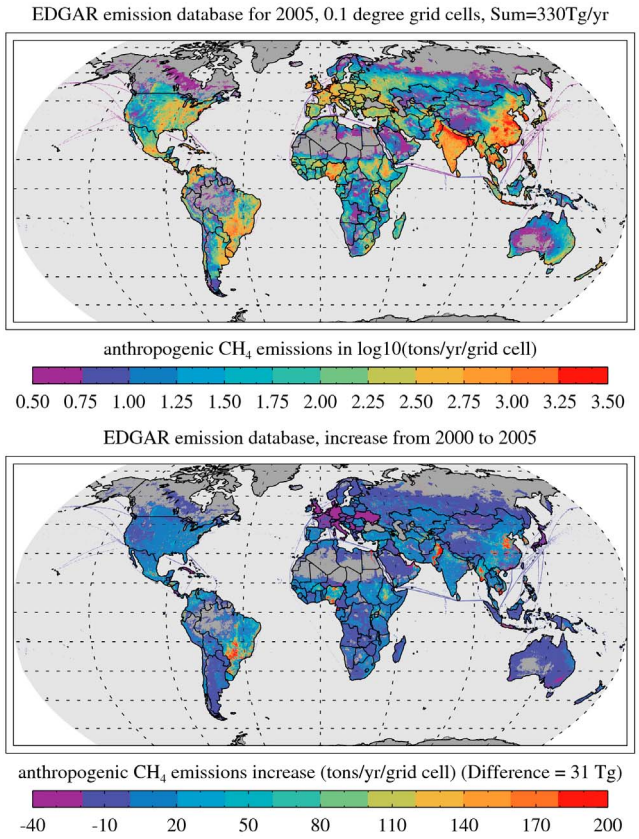

Figure 13. (top) Anthropogenic methane emission estimates from the Emission Database for Global Atmospheric Research (EDGAR) database. (Note the log scale.) (bottom) Difference in anthropogenic methane emissions between 2000 and 2005. Source is the European Commission, Joint Research Centre (JRC)/Netherlands Environmental Assessment Agency (PBL) EDGAR, release version 4.0, 2009 (available at http://edgar.jrc.ec.europe.eu/).

nounced peaks at the end of 2007 and beginning of 2008. East Asia is the only region where both SCIAMACHY and the TM5 model confirm a positive anomaly in the time period of interest, namely, from August through November 2006, shortly before the large-scale increase starting in January 2007.

[27] Even though it may be unsatisfying at this stage, we cannot yet draw strong conclusions on the basis of the observations from SCIAMACHY alone. A tentative conclusion is that it is unlikely that the increase in 2007 through 2009 was caused by an increase of methane emissions in a single and very specific region not detectable by ground-based stations. Since the increase was observed in both hemispheres at about the same time, a dramatic increase of high-latitude wetland emissions in each of the years can be excluded as the sole explanation. Tropical regions and East Asian areas that are sometimes located south of the ITCZ are the most suitable candidates as they emit into both hemispheres. Regional anomalies reported here can also be caused by anomalies in wind patterns or tropopause height or clouds, making the application of global chemistry transport models for source inversions indispensable. Further investigations applying this data set in conjunction with all ground-based stations in an inverse model are thus necessary to shed light on the observed anomaly and potential culprits. A prerequisite for this, however, is a consistent and long-term data set, which, in the case of SCIAMACHY, was much harder to achieve than previously anticipated.

6. Bottom-Up Inventories of Anthropogenic Emissions

[28] Almost as surprising as the increase starting in 2007 is the fact that we saw stabilizing methane abundances after 1999 through 2006 [*Dlugokencky et al.*, 2003]. From 2000 to 2005, the Emission Database for Global Atmospheric Research (EDGAR) posits an increase in annual anthropogenic emissions of about 31 Tg, more than is needed to explain the anomaly starting in 2007. This raises the question, Why have we not observed a continuing increase in global methane abundance? *Bousquetet al.* [2006] analyzed this phenomenon using ground-based methane observations and stated that increasing anthropogenic methane emissions are offset by decreasing wetland emission. As *Bousquet et al.* [2006] stated (shortly before the methane increase), increasing global emissions can be expected just by wetland emissions going back to normal. This may be a potential explanation, but there is, to the best of our knowledge, no climatic anomaly that might trigger a dramatic change in wetland emissions persistently from 2007 through 2009.

[29] Figure 13 shows high-resolution bottom-up inventories of anthropogenic methane emissions provided by the EDGAR database. Figure 13 (bottom) depicts the change between 2000 and 2005, summing to a total increase in annual emissions of 32 Tg, half of which is attributed to areas between 20°N and 40°N. However, many changes in the EDGAR database are percentage shifts of individual countries and should thus be interpreted with care.

7. High-Resolution Regional Averages of Multiyear Column-Averaged Methane Mixing Ratios

[30] One of the advantages of space-based observations is the ability to sense trace gases globally with the same instrument. Even though an extensive ground-based network spanning all regions of the globe at reasonable scales might in principle provide a similar reduction of uncertainties in global flux estimates, in many regions the establishment of a ground-based network may be hard to implement. This can be due to political instability or simply naturally inaccessible areas (which would actually be the most interesting ones with respect to natural fluxes). Several studies have shown and quantified [*Rayner and O'Brien*, 2001; *Houweling et al.*, 2004; *Chevallier et al.*, 2007; *Miller et al.*, 2007] the potential of accurate spaceborne greenhouse gas measurements in regard to flux uncertainty reductions on regional scales. There is, however, a further benefit which may be harder to quantify: The detection of small-scale hot spots in the global distribution and subsequent dedicated ground-based measurements for verification

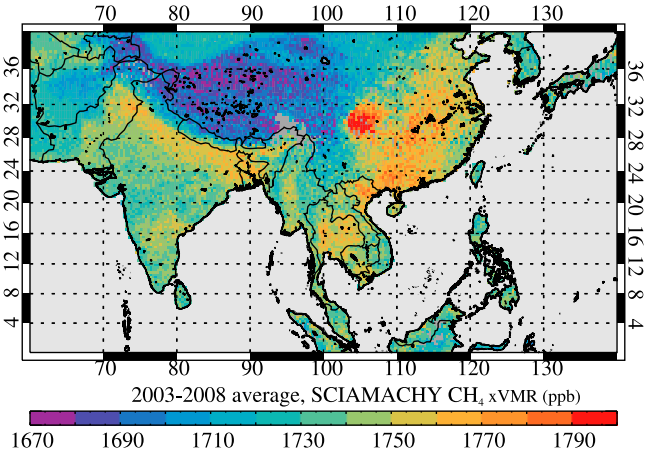

Figure 14. High spatial resolution 6 year average (2003 through 2008) of SCIAMACHY xCH_4 over eastern Asia. Gridding has been performed on 1/3° by 1/3° dimensions without additional spatial smoothing (i.e., pixels do not share information from the same SCIAMACHY measurements).

of observed anomalies and determination of the type of sources.

[31] The long-term data set of SCIAMACHY now enables the calculation of global averages at a fine spatial resolution. In the following discussion, we present several regions on Earth with a focus on landmasses. All plots have been gridded to 1/3° by 1/3°, and the average within a grid box is constituted by all retrievals within this time period where the center of the SCIAMACHY ground pixel falls within the grid box. (That is, neighboring grid boxes do not share any information from retrievals with each other, and it is important to note that no spatial smoothing has been applied.) Most figures are self-explanatory, and we thus refrain from lengthy descriptions. The impact of regional scale elevation changes, however, should be always kept in mind when interpreting the long-term averages.

[32] Figure 14 shows the long-term average over Asia. The prominent feature in Asia is the Red Basin in China, exhibiting, on average, the highest methane column averages on Earth. While emissions from rice paddies, agriculture, and industrial processes might indeed be very high in this region, it may be premature to deduct the highest flux

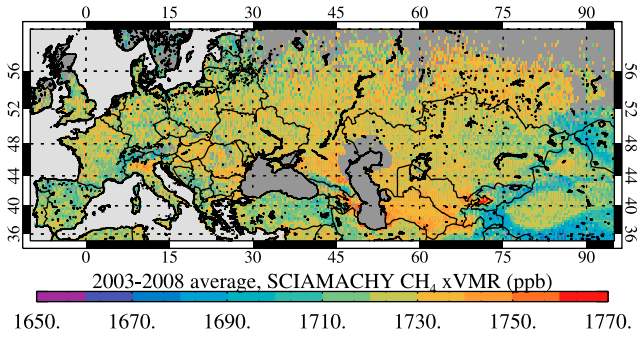

Figure 15. Same as Figure 14 but for Europe and western Asia.

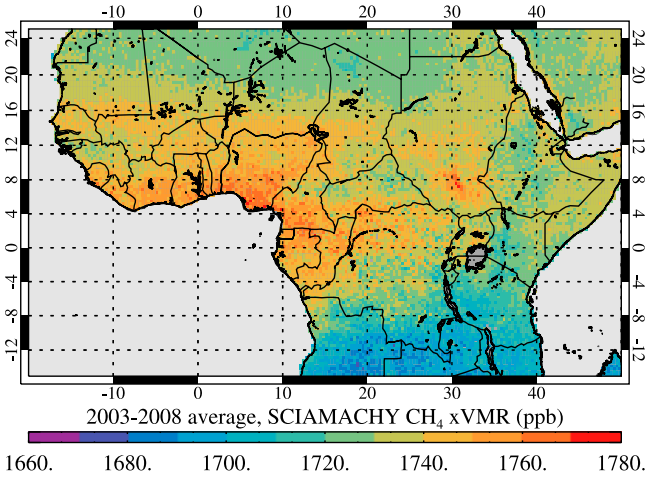

Figure 16. Same as Figure 14 but for tropical Africa.

rates in this region as the basin structure potentially causes longer atmospheric residence times. Also, the EDGAR emission database posits very high emissions from this region (see Figure 13). Another prominent feature in Asia, also consistent with high anthropogenic emissions as stated by EDGAR, are the Gangetic Plains, with relatively high methane abundance most likely caused by rice paddies, wetlands, and high ruminant density. (Wetlands are not in the EDGAR database.) The sharp boundary at the foothills of the Himalayas is largely an elevation effect, causing lower total column averages due to the fact that the stratosphere contributes more strongly to the total column in that case.

[33] Figure 15 shows Eurasia, and several interesting features can be observed, the most striking being the Fergana Valley in Uzbekistan. Over this region, *Clarisse et al.* [2009] observed elevated levels of ammonia, pointing to intense agricultural activity. Similar to the Red Basin, however, the valley structure might cause part of the elevated levels. Also, around the Caspian Sea, enhanced

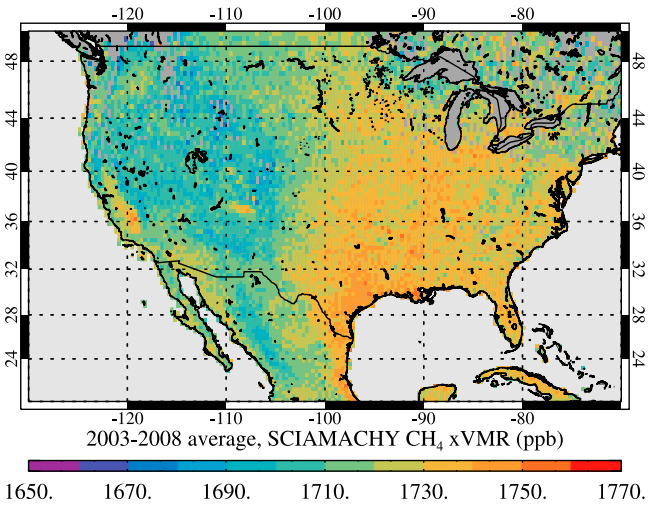

Figure 17. Same as Figure 14 but for North America.

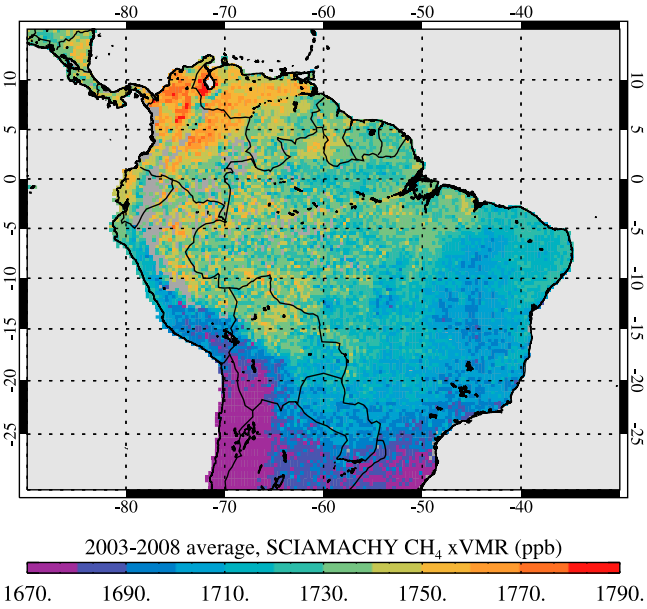

Figure 18. Same as Figure 14 but for tropical South America.

methane abundance correlating with spatial patterns of predicted anthropogenic emissions can be observed (most strikingly in Azerbaijan).

[34] In tropical Africa (Figure 16), the Sudd wetland region in southern Sudan clearly stands out as a very localized methane source. Also, land regions around the Gulf of Guinea exhibit higher values than the long-term average.

[35] In North America (Figure 17), the Rocky Mountains cause a strong difference between the eastern and western parts, again just due to an elevation effect. The San Joaquin Valley in California exhibits enhanced methane abundance in the western United States, most likely caused by agriculture and the elevation effect.

[36] In South America (Figure 18), the north-south gradient is a dominant feature, while the northernmost part exhibits the highest column-averaged mixing ratios on average. One reason for the high abundance in this region is that it is mostly located north of the ITCZ, thus making it subject to higher background concentrations. Furthermore, very high column mixing ratios are retrieved around Lake Maracaibo. The EDGAR database states total annual emissions of about 5.7 Tg for Colombia and Venezuela together, primarily from fugitive emissions and enteric fermentation. According to Figure 13, most of these emissions are located in the northernmost parts, which would fit our observations.

8. Discussion and Conclusion

[37] We have analyzed SCIAMACHY xCH_4 retrieval from 2003 through 2009 using the CO_2 proxy approach [*Frankenberg et al.*, 2005]. A serious degradation of crucial detector pixels at the end of 2005 was observed and prompted us to flag those detector pixels as bad for the entire time period. This reduces the overall quality of retrieval and causes small systematic differences compared with the previous retrieval version [*Frankenberg et al.*, 2008a]. However, it enables a more consistent analysis of long-term behavior. In agreement with the ground-based measurement network, we observe a small decrease in global methane abundance until the end of 2006, followed by a consistent increase until the end of the period of investigation. We find that deseasonalized time series of SCIAMACHY methane correspond well with ground-based observations, especially over the Sahara, where ideal comparison conditions are met. In SCIAMACHY retrievals, we observe a negative anomaly of tropical abundance (more pronounced in Africa than in South America) in 2006, but we cannot yet fully exclude a retrieval bias due to degradation. Over East Asia, a positive anomaly from August through November 2006 can be seen and is consistent with TM5 model simulations. However, we cannot yet draw strong conclusions as to the origin of the methane anomaly on the basis of methane observations alone. Future research using SCIAMACHY and ground-based data in source inversions is indispensable to providing a more quantitative and robust answer to this question.

[38] We further present long-term averages of SCIAMACHY retrievals gridded on a very fine spatial resolution with zoom over key regions. Many emission hot spots such as the Red Basin in China, the Gangetic Plains in India, areas around Lake Maracaibo in Venezuela, or the Sudd wetlands in Sudan can be observed. Distinct spatial gradients observed here can also be very useful in defining regions of interest for more focused ground-based research.

[39] To conclude, none of the anomalies observed in the past 25 years [*Dlugokencky et al.*, 2003] have lasted this long, and this definitely renders the current anomaly as special. However, at present, it remains unclear whether the increased mixing ratios since 2007 represent an anomaly or indicate the beginning of a new period of increasing CH_4 mixing ratios. Besides long-term trends of anthropogenic emissions (being different in different world regions) and interannual variations and trends of natural emissions (wetlands), the OH sink also may play some role.

[40] **Acknowledgments.** CF was mostly supported by the Dutch Science Foundation (NWO) through a VENI grant. We acknowledge John Burrows, PI of the SCIAMACHY instrument, for having initiated and realized the SCIAMACHY project. The Netherlands SCIAMACHY Data Center and ESA are greatly appreciated for providing data. We thank Wouter Peters for providing CarbonTracker results and A. Segers, C. Schrijvers, O. Tuinder, and A. Gloudemans for providing ECMWF data collocated with SCIAMACHY. We acknowledge the European Commission for supporting the Sixth Framework Programme project HYMN (contract 037048) and GEOMON (contract 036677), GEMS-IP (contract SIP4-CT-2004-516099). We further acknowledge exchange of information within the EU 6th FP Network of Excellence ACCENT. The research leading to these results has received funding from the European Union's Seventh Framework Programme (FP7/2007–2013) under Grant Agreement 218793. Part of the research was funded through the EU's Seventh Framework Programme (FP7/2007–2013) under Grant Agreement 218793 (MACC). We further acknowledge the source of EDGAR data: European Commission, Joint Research Centre (JRC)/Netherlands Environmental Assessment Agency (PBL); Emission Database for Global Atmospheric Research (EDGAR), release version 4.0 (http://edgar.jrc.ec.europa.eu), 2009. We thank and honor Annemieke Gloudemans, who provided ancillary data and continued the work started in this paper. Her unexpected death is a tragic loss to all of us.

References

Bergamaschi, P., et al. (2007), Satellite chartography of atmospheric methane from SCIAMACHY on board Envisat: 2. Evaluation based on

inverse model simulations, *J. Geophys. Res.*, *112*, D02304, doi:10.1029/2006JD007268.

Bergamaschi, P., et al. (2009), Inverse modeling of global and regional CH_4 emissions using SCIAMACHY satellite retrievals, *J. Geophys. Res.*, *114*, D22301, doi:10.1029/2009JD012287.

Bergamaschi, P., et al. (2010), Inverse modeling of European CH_4 emissions 2001–2006, *J. Geophys. Res.*, *115*, D22309, doi:10.1029/2010JD014180.

Bloom, A., P. Palmer, A. Fraser, D. Reay, and C. Frankenberg (2010), Large-scale controls of methanogenesis inferred from methane and gravity spaceborne data, *Science*, *327*(5963), 322–325.

Bousquet, P., et al. (2006), Contribution of anthropogenic and natural sources to atmospheric methane variability, *Nature*, *443*(7110), 439–443.

Butz, A., O. Hasekamp, C. Frankenberg, J. Vidot, and I. Aben (2010), CH_4 retrievals from space-based solar backscatter measurements: Performance evaluation against simulated aerosol and cirrus loaded scenes, *J. Geophys. Res.*, *115*, D24302, doi:10.1029/2010JD014514.

Chevallier, F., F.-M. Bréon, and P. J. Rayner (2007), Contribution of the Orbiting Carbon Observatory to the estimation of CO_2 sources and sinks: Theoretical study in a variational data assimilation framework, *J. Geophys. Res.*, *112*, D09307, doi:10.1029/2006JD007375.

Clarisse, L., C. Clerbaux, F. Dentener, D. Hurtmans, and P.-F. Coheur (2009), Global ammonia distribution derived from infrared satellite observations, *Nat. Geosci.*, *2*, 479–483, doi:10.1038/ngeo551.

Dlugokencky, E., S. Houweling, L. Bruhwiler, K. Masarie, P. Lang, J. Miller, and P. Tans (2003), Atmospheric methane levels off: Temporary pause or a new steady-state, *Geophys. Res. Lett.*, *30*(19), 1992, doi:10.1029/2003GL018126.

Dlugokencky, E., et al. (2009), Observational constraints on recent increases in the atmospheric CH_4 burden, *Geophys. Res. Lett.*, *36*, L18803, doi:10.1029/2009GL039780.

Forster, P., et al. (2007), Changes in atmospheric constituents and in radiative forcing, in *Climate Change 2007: The Physical Science Basis. Working Group I Report*, edited by S. Solomon et al., pp. 131–234, Cambridge Univ. Press, New York.

Frankenberg, C., J. F. Meirink, M. van Weele, U. Platt, and T. Wagner (2005), Assessing methane emissions from global space-borne observations, *Science*, *308*(5724), 1010–1014, doi:10.1126/science.1106644.

Frankenberg, C., J. F. Meirink, P. Bergamaschi, A. P. H. Goede, M. Heimann, S. Körner, U. Platt, M. van Weele, and T. Wagner (2006), Satellite chartography of atmospheric methane from SCIAMACHY on board Envisat: Analysis of the years 2003 and 2004, *J. Geophys. Res.*, *111*, D07303, doi:10.1029/2005JD006235.

Frankenberg, C., et al. (2008a), Tropical methane emissions: A revised view from SCIAMACHY onboard Envisat, *Geophys. Res. Lett.*, *35*, L15811, doi:10.1029/2008GL034300.

Frankenberg, C., et al. (2008b), Pressure broadening in the $2\nu_3$ band of methane and its implication on atmospheric retrievals, *Atmos. Chem. Phys.*, *8*(17), 5061–5075.

Hoogeveen, R., R. van der A, and A. Goede (2001), Extended wavelength InGaAs infrared (1.0–2.4 μm) detector arrays on SCIAMACHY for space-based spectrometry of the Earth atmosphere, *Infrared Phys. Technol.*, *42*(1), 1–16.

Houweling, S., F. Bréon, I. Aben, C. Rodenbeck, M. Gloor, M. Heimann, and P. Ciais (2004), Inverse modeling of CO_2 sources and sinks using satellite data: A synthetic inter-comparison of measurement techniques and their performance as a function of space and time, *Atmos. Chem. Phys.*, *4*, 523–538.

Kleipool, Q., R. Jongma, A. Gloudemans, H. Schrijver, G. Lichtenberg, R. van Hees, A. Maurellis, and R. Hoogeveen (2007), In-flight proton-induced radiation damage to SCIAMACHY's extended-wavelength InGaAs near-infrared detectors, *Infrared Phys. Technol.*, *50*(1), 30–37.

Krol, M., S. Houweling, B. Bregman, M. van den Broek, A. Segers, P. van Velthoven, W. Peters, F. Dentener, and P. Bergamaschi (2005), TM5, a global two-way nested chemistry transport zoom model: Algorithm and applications, *Atmos. Chem. Phys*, *5*, 417–432.

Kuze, A., H. Suto, M. Nakajima, and T. Hamazaki (2009), Thermal and near infrared sensor for carbon observation Fourier-transform spectrometer on the Greenhouse Gases Observing Satellite for greenhouse gases monitoring, *Appl. Opt.*, *48*(35), 6716–6733.

Lelieveld, J., P. Crutzen, and F. Dentener (1998), Changing concentration, lifetime and climate forcing of atmospheric methane, *Tellus, Ser. B*, *50*(2), 128–150.

Meirink, J., P. Bergamaschi, and M. Krol (2008), Four-dimensional variational data assimilation for inverse modelling of atmospheric methane emissions: Method and comparison with synthesis inversion, *Atmos. Chem. Phys*, *8*, 6341–6353.

Miller, C. E., et al. (2007), Precision requirements for space-based X-CO_2 data, *J. Geophys. Res.*, *112*, D10314, doi:10.1029/2006JD007659.

Peters, W., et al. (2007), An atmospheric perspective on North American carbon dioxide exchange: CarbonTracker, *Proc. Natl. Acad. Sci. U. S. A.*, *104*(48), 18,925–18,930, doi:10.1073/pnas.0708986104.

Rayner, P., and D. O'Brien (2001), The utility of remotely sensed CO_2 concentration data in surface source inversions, *Geophys. Res. Lett.*, *28*(1), 175–178, doi:10.1029/2000GL011912.

Rigby, M., et al. (2008), Renewed growth of atmospheric methane, *Geophys. Res. Lett.*, *35*, L22805, doi:10.1029/2008GL036037.

Schneising, O., M. Buchwitz, J. P. Burrows, H. Bovensmann, P. Bergamaschi, and W. Peters (2009), Three years of greenhouse gas column-averaged dry air mole fractions retrieved from satellite. Part 2: Methane, *Atmos. Chem. Phys.*, *9*(2), 443–465.

Sheather, S., and M. Jones (1991), A reliable data-based bandwidth selection method for kernel density estimation, *J. R. Stat. Soc., Ser. B*, *53*(3), 683–690.

I. Aben, R. van Hees, S. Houweling, R. Snel, P. Tol, and P. van der Meer, SRON Netherlands Institute for Space Research, Sorbonnelaan 2, NL-3584 CA Utrecht, Netherlands.

P. Bergamaschi, Institute for Environment and Sustainability, European Commission Joint Research Centre, TP 290, I-21020 Ispra, Italy.

E. J. Dlugokencky, NOAA Earth System Research Laboratory, Global Monitoring Division, 325 Broadway, Boulder, CO 80305, USA.

C. Frankenberg, Jet Propulsion Laboratory, California Institute of Technology, 4800 Oak Grove Drive, Pasadena, CA 91109, USA. (christian.frankenberg@jpl.nasa.gov)